ADVANCED ENERGY MATERIALS

Supporting Information

for *Adv. Energy Mater.,* DOI: 10.1002/aenm.202201469

Converting Brownmillerite to Alternate Layers of Oxygen-Deficient and Conductive Nano-Sheets with Enhanced Thermoelectric Properties

Songbai Hu, Wenqiao Han, Xiaowen Li, Mao Ye, Yao Lu, Cai Jin, Qi Liu, Junling Wang, Jiaqing He, Claudio Cazorla, Yuanmin Zhu, and Lang Chen**

Supporting Information

Converting brownmillerite to alternate layers of oxygen-deficient and conductive nano-sheets with enhanced thermoelectric properties

Songbai Hu, Wenqiao Han, Xiaowen Li, Mao Ye, Yao Lu, Cai Jin, Qi Liu, Junling Wang, Jiaqing He, Claudio Cazorla, Yuanmin Zhu, Lang Chen**

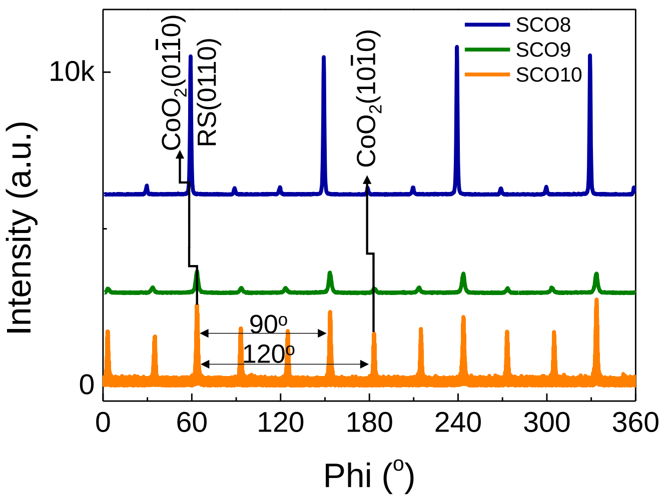

Figure S1. XRD in-plane phi-scan for SCO10, SCO9 and SCO8 along RS (110) and $CoO_2(01\bar{1}0)$ directions.

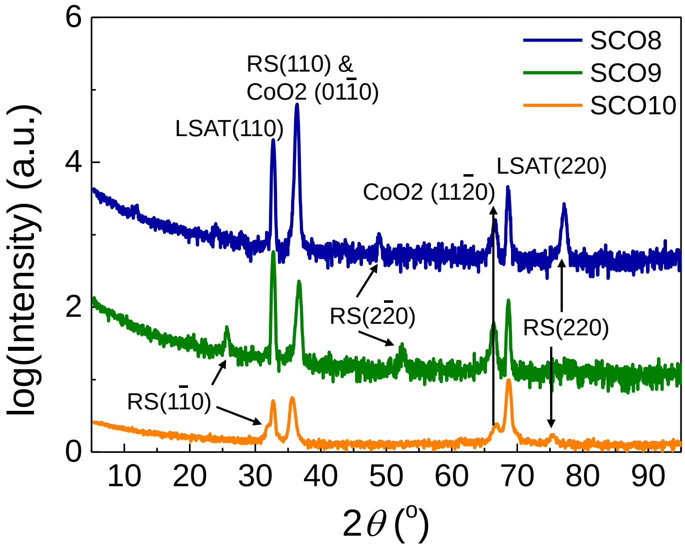

Figure S2. XRD in-plane *θ*-2*θ* scans for SCO10, SCO9 and SCO8 along LSAT (110) direction.

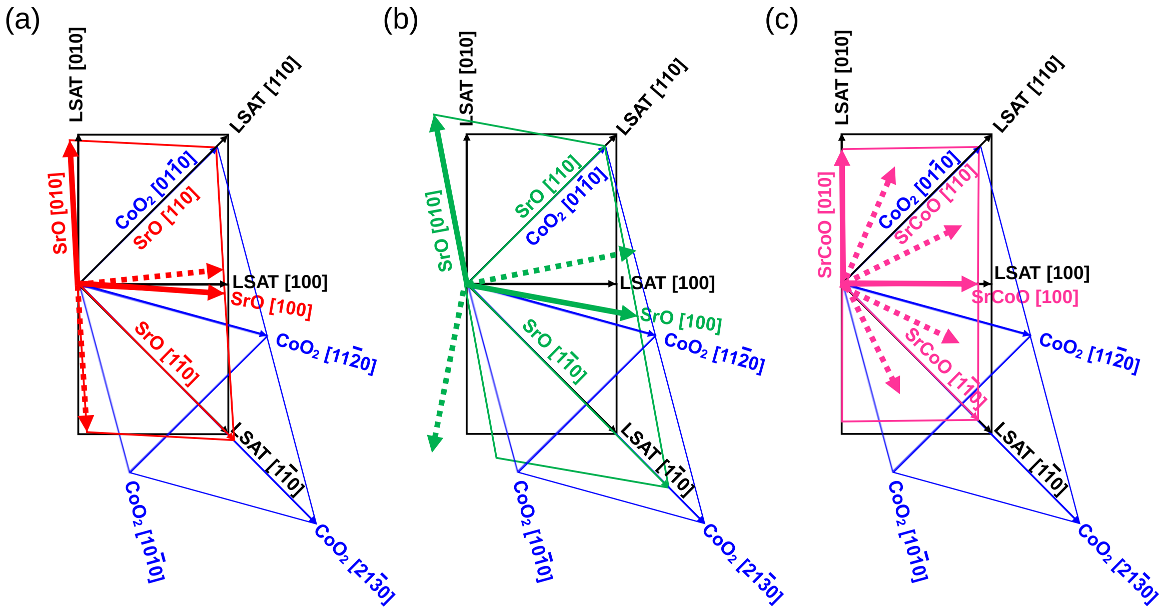

Figure S3. The in-plane epitaxial relationships between (a) SCO10, (b) SCO9 and (c) SCO8 thin films and the LSAT substrate. The dashed arrows depict the rotatory counterparts of the rock salt Sr_2O_2(SrO)/Sr_2CoO_3(SrCoO) layer.

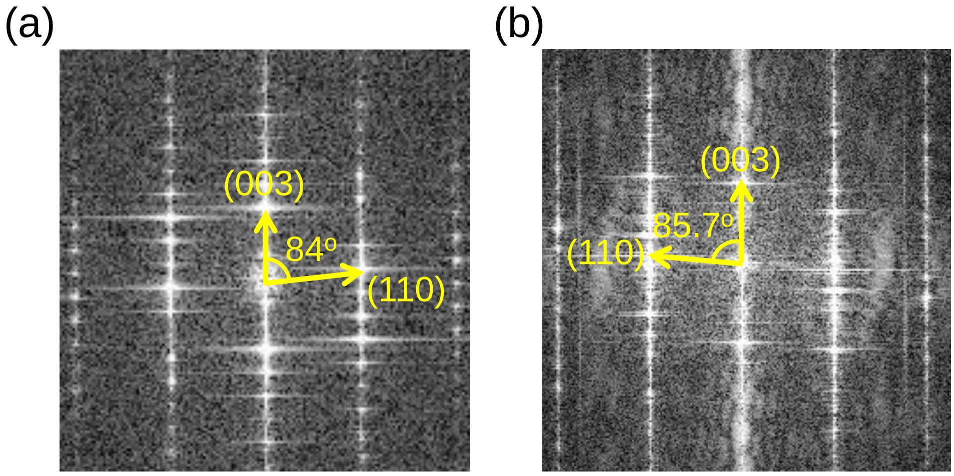

Figure S4. Fast flourier transformation (FFT) of the (a) SCO9 (110) atomic plane and (b) SCO8 (110) plane.

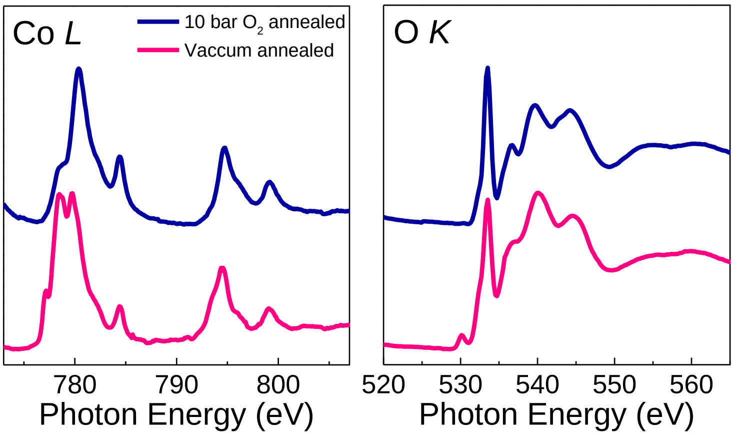

Figure S5. XAS of Co *L*-edge and O *K*-edge for vacuum or 10 bar O_2 annealed SCO10 thin films. The XAS near Co *L*-edge confirmed the presence of Co^{2+} in vacuum-annealed SCOH thin film as seen the peak splitting near 780 eV. As the Co^{2+} was oxidized to Co^{3+} in 10 bar O_2, the Co^{2+} splitting in the left panel was highly suppressed. Correspondingly, a clear bump at 530 eV was detected in the O *K*-edge spectrum for vacuum annealed SCO10. However, this bump was undetectable in the 10 bar O_2 annealed sample. Therefore, the bump represents the electronic transition from a O 2*p* state to the half-filled a_{1g} state of the hybridized orbital Co^{II} 3*d*-O 2*p* in oxygen deficient SCO10.

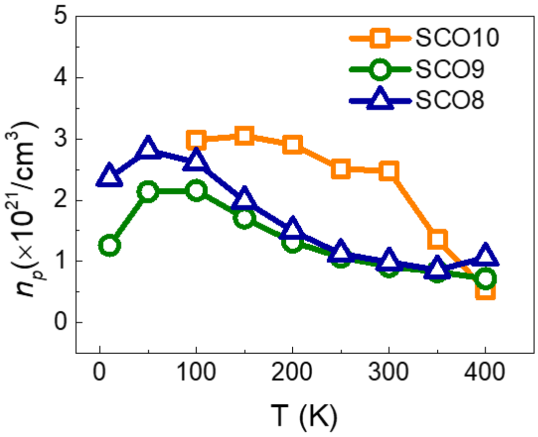

Figure S6. Carrier concentration (n_p) of SCO10, SCO9 and SCO over the temperature interval 10 K ~ 400 K.

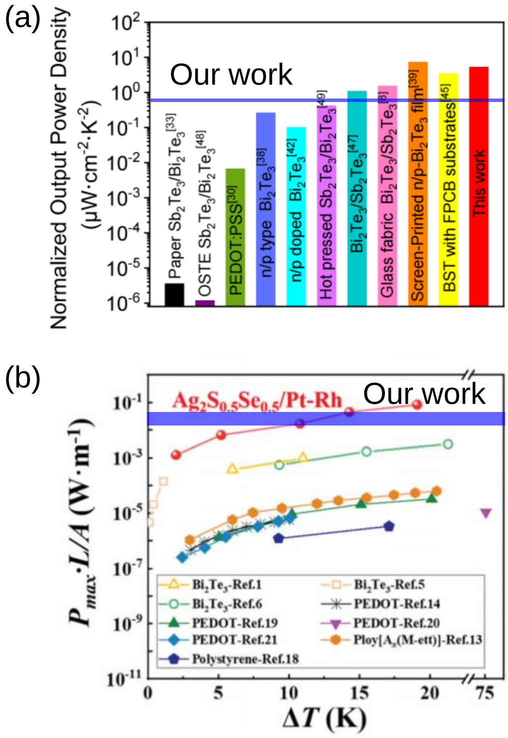

Figure S7. Reported normalized power density for Bi_2Te_3-based thermoelectric films in (a) reference [40] and (b) reference [41] of main text. The light-blue bar dictates the range span for our SCO9 thin film.

Reproduced with permission [40]. Copyright 2022, Elsevier.
Reproduced with permission [41], Copyright 2019, Royal Society of Chemistry.

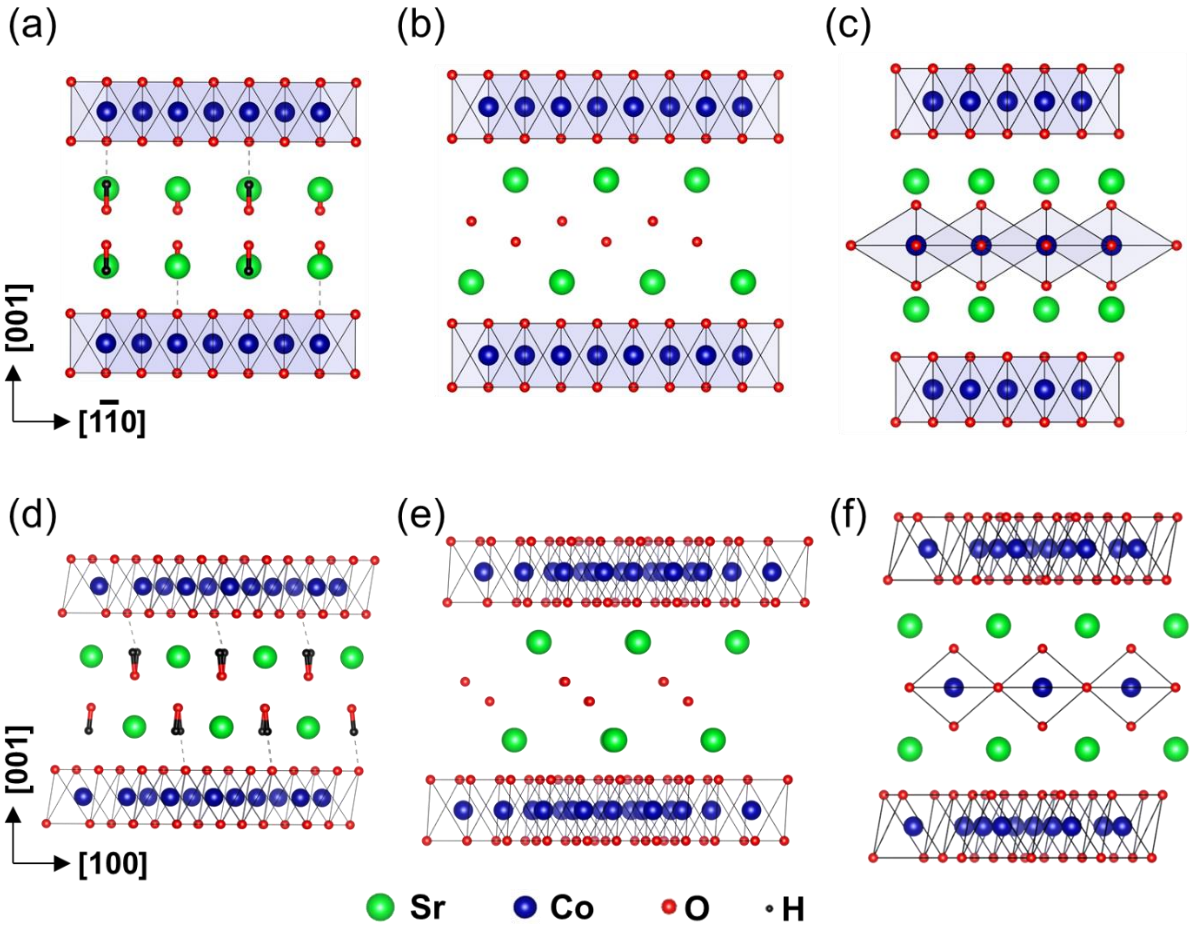

Figure S8. (1$\bar{1}$0) atomic plane for (a) SCO10, (b) SCO9 and (c) SCO8 and (100) atomic plane for (d) SCO10, (e) SCO9 and (f) SCO8

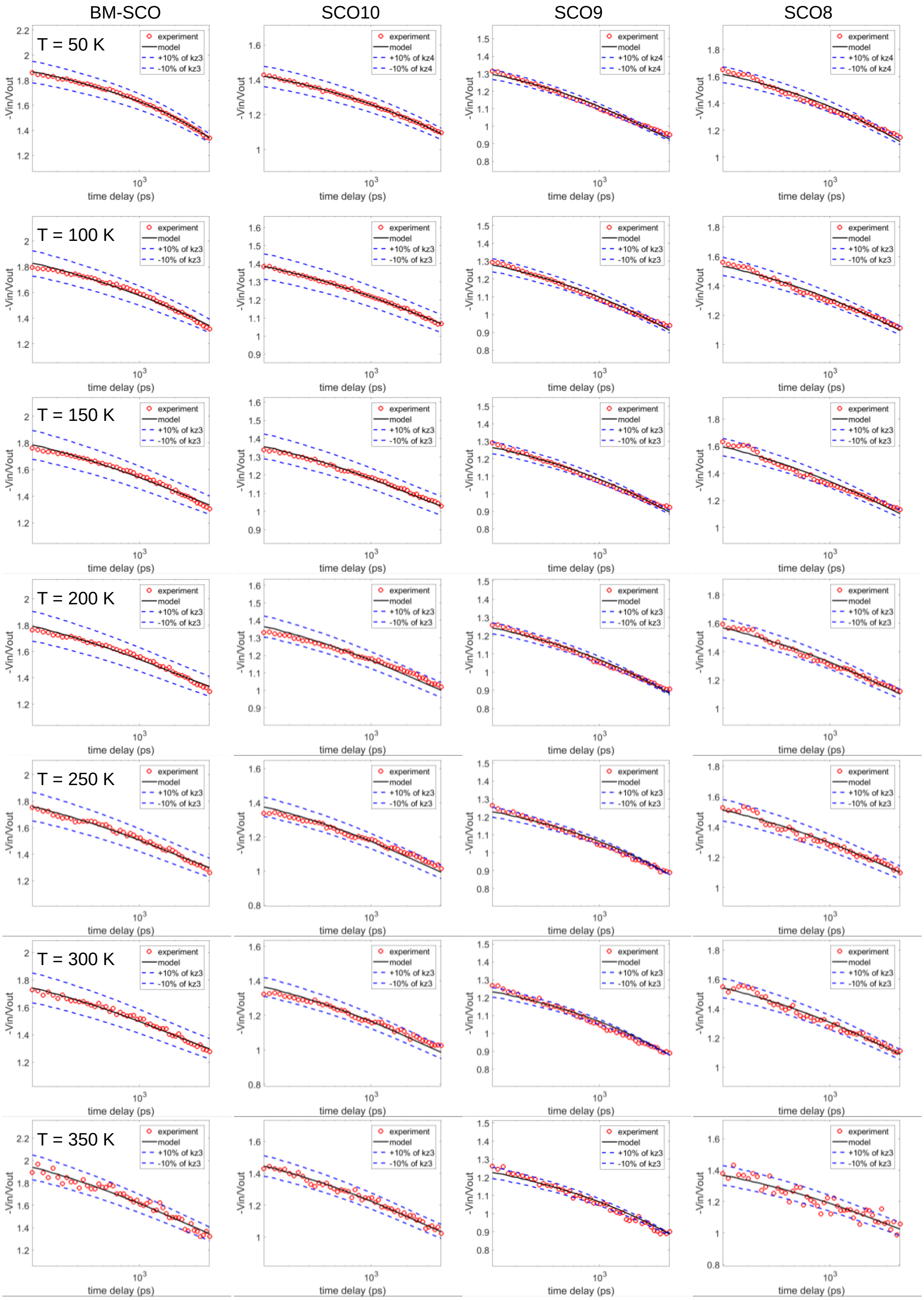

Figure S9. The plots of -V_{in}/V_{out} vs. delay time for SCO thin films at different temperature obtained from TDTR. The experiment raw data, curves fitted with optimum and 10% uncertainties of κ were represented by open circles, solid lines and dash lines, respectively.

Table S1. Resistivity (ρ), Seebeck coefficient (*S*) and power factors (*PF*) of several thermoelectrical materials near room temperature

	ρ [mΩ cm]	*S* [μVK^{-1}]	*PF* [10^{-4} WK^{-2}m]	Ref.
$Ca_3Co_4O_9$ (thin film)	14.2	200	2.8	[1]
$Ca_3Co_4O_9$ (powder)	12.6	~92	0.67	[2]
$Ca_3Co_4O_9$ (crystal)	11	~125	1.4	[3]
$Ca_2Co_2O_5$	1.4	137	13.4	[4]
$Sr_3Co_4O_9$	2.5	95	3.6	[5]
Ge doped $[Sr_2CoO_3][CoO_2]_{1.8}$	130	~110	0.09	[6]
$NaCo_2O_4$	0.2	100	50	[7]
Nb doped $SrTiO_3$	5.9	-97	1.6	[8]
La doped $SrTiO_3$	1	-150	23	[9]
$Sr_3Ti_2O_7$	5.1	-86	1.5	[8]
$Zn_{0.95}Al_{0.05}O$	~52	~-170	15	[10, 11]
$(ZnO)_5In_2O_3$	0.065	-9.6	1.4	[12]
Bi_2Te_3	1	200	40	[7]
Sb_2Te_3	0.36	135	52	[13]
BM-$SrCoO_{2.5}$	13438	112	0.0009	Our work
$[Sr_2O_2H_2]_{0.5}CoO_2$	1.74	128	9.4	Our work
$[Sr_2O_2]_{0.4}CoO_2$	0.27	98	35.7	Our work
$[Sr_2CoO_3]_{0.57}CoO_2$	0.37	90	21.9	Our work

References

[1] B. Paul, E. M. Bjork, A. Kumar, J. Lu, P. Eklund, *ACS Appl. Energy Mater.* 2018, **1**, 2261.

[2] S. W. Li, R. Funahashi, I. Matsubara, K. Ueno, H. Yamada, *J. Mater. Chem.* 1999, **9**, 1659.

[3] A. C. Masset, C. Michel, A. Maignan, M. Hervieu, O. Toulemonde, F. Studer, B. Raveau, J. Hejtmanek, *Phys. Rev. B* 2000, **62**, 166.

[4] R. Funahashi, I. Matsubara, H. Ikuta, T. Takeuchi, U. Mizutani, S. Sodeoka, *Jpn. J. Appl. Phys., Part 2* 2000, **39**, L1127.

[5] A. Sakai, T. Kanno, S. Yotsuhashi, A. I. Odagawa, H. Adachi, Ieee, "Preparation and anisotropic thermoelectric properties in misfit cobaltite thin films", presented at *24th International Conference on Thermoelectrics (ICT)*, Clemson, SC, Jun 19-23, 2005.

[6] D. Pelloquin, S. Hébert, A. Maignan, B. Raveau, *Solid State Sci.* 2004, **6**, 167.

[7] I. Terasaki, Y. Sasago, K. Uchinokura, *Phys. Rev. B* 1997, **56**, 12685.

[8] K. Koumoto, I. Terasaki, R. Funahashi, *MRS Bull.* 2006, **31**, 206.

[9] S. Ohta, T. Nomura, H. Ohta, K. Koumoto, *J. Appl. Phys.* 2005, **97**.

[10] M. Ohtaki, T. Tsubota, K. Eguchi, H. Arai, *J. Appl. Phys.* 1996, **79**, 1816.

[11] T. Tsubota, M. Ohtaki, K. Eguchi, H. Arai, *J. Mater. Chem.* 1997, **7**, 85.

[12] H. Ohta, W. S. Seo, K. Koumoto, *J. Am. Ceram. Soc.* 1996, **79**, 2193.

[13] S. Shen, W. Zhu, Y. Deng, H. Zhao, Y. Peng, C. Wang, *Appl. Surf. Sci.* 2017, **414**, 197.

Table S2. T_{high} and T_{low} during the output power measurement.

	Hot plate setup [°C]	T_{high} [°C]	T_{low} [°C]	T_{high}-T_{low} [K]	ΔT estimated by V_{oc}/S [K]
SCO10	50	41	31	12	14
	70	51	36	15	18
	90	59	38	21	23
SCO9	50	41	29	12	14
	70	53	34	19	21
	90	65	40	25	28
SCO8	50	46	32	14	17
	70	56	34	22	24
	90	70	40	30	33